RESEARCH

ROS-induced near-homozygous genomes in thyroid cancer

Willem E Corver, Joris Demmers, Jan Oosting, Shima Sahraeian, Arnoud Boot, Dina Ruano, Tom van Wezel and **Hans Morreau**

Department of Pathology Leiden University Medical Center, Leiden, Netherlands

Correspondence should be addressed to W E Corver or H Morreau: w.e.corver@lumc.nl or j.morreau@lumc.nl

Abstract

A near-homozygous genome (NHG) is especially seen in a subset of follicular thyroid cancer of the oncocytic type (FTC-OV). An NHG was also observed in the metabolically relatively quiescent cell lines XTC.UC1, a model for FTC-OV, and in FTC-133, -236 and -238, the latter three derived from one single patient with follicular thyroid cancer. FTC-236 subclones showed subtle whole-chromosome differences indicative of sustained reciprocal mitotic missegregations. Reactive oxygen species (ROS) scavenger experiments reduced the number of chromosomal missegregations in XTC.UC1 and FTC-236, while pCHK2 was downregulated in these cells. Treatment with antimycin A increased ROS indicated by enhanced MitoSOX Red and pCHK2 fluorescence in metaphase cells. In a selected set of oncocytic follicular thyroid tumors, increasing numbers of whole-chromosome losses were observed toward an aggressive phenotype, but with retention of chromosome 7. Together, ROS activates CHK2 and links to the stepwise loss of whole chromosomes during tumor progression in these lesions. We postulate that sequential loss of whole chromosomes is a dominant driver of the oncogenesis of a subset of follicular thyroid tumors.

Key Words

- thyroid neoplasm
- oncocytic
- reactive oxygen species
- chromosome instability
- checkpoint kinase 2

Endocrine-Related Cancer (2018) **25**, 83–97

Introduction

Follicular thyroid cancer of the oncocytic variant (FTC-OV) is overrepresented in recurrent non-medullary thyroid cancer (NMTC) (Wada *et al.* 2002). FTC-OV is characterized by a strong eosinophilic cytoplasm due to abundant mitochondria in conjunction with a reprogrammed metabolism probably driven by estrogen-related receptor α (Mirebeau-Prunier *et al.* 2013). In FTC-OV mitochondrial DNA (mtDNA), variants in complexes of the respiratory chain are also found, which might cause a restricted ATP production (Bonora *et al.* 2006). Nonetheless, disruptive and/or damaging mtDNA variants are not exclusive to oncocytic tumors, since these mutations were as frequently found in non-oncocytic papillary thyroid and other cancers (Chatterjee *et al.* 2006, Zhou *et al.* 2007, Larman *et al.* 2012, Ju *et al.* 2014).

FTC-OV has been extensively studied at the genomic level (Maximo *et al.* 2014). Based upon flow or image DNA cytometry, comparative genomic hybridization (CGH) experiments or interphase fluorescence *in situ* hybridization, these tumors were considered diploid or aneuploid with whole-chromosome gains (McLeod *et al.* 1988, Flint & Lloyd 1990, Salmon *et al.* 1993, Roque *et al.* 1999, Tallini *et al.* 1999, Erickson *et al.* 2001, Wada *et al.* 2002, Dettori *et al.* 2003). Using a new method for DNA content analysis (Corver *et al.* 2005) in combination with single nucleotide polymorphism (SNP) technology

http://erc.endocrinology-journals.org
https://doi.org/10.1530/ERC-17-0288

(Corver *et al*. 2008), we demonstrated that many FTC-OV actually show a near-homozygous genome (NHG) in which a phase of near-haploidization is followed by endoreduplication or genome doubling of the entire NHG (Corver *et al*. 2012, 2014). Our observations regarding an NHG have been confirmed by others (Wagle *et al*. 2014, Kasaian *et al*. 2015). Furthermore, retention of chromosome 7, a hallmark for FTC-OV, was recently attributed to genomic imprinting of genes on both paternal and maternal alleles that are important for tumor cell survival (Boot *et al*. 2016).

The loss of many entire chromosomes (whole-chromosome instability, w-CIN) as found in tumors with an NHG suggests chromosome missegregations or non-disjunctions during mitosis. Despite the fact that molecular mechanisms implicated in w-CIN are studied extensively, a common cause in cancer has so far not been found.

Recently, Bakhoum and coworkers demonstrated that doxorubicin or ionizing radiation (IR) during mitosis induced a DNA damage response with lagging chromosomes (Bakhoum *et al*. 2014). Exposing cells to chloroquine, an activator of ATM-kinase, induced lagging chromosomes to the same levels but without significant DNA damage. ATM can also be activated by oxidative stress in the absence of DNA double-strand breaks (Alexander *et al*. 2010, Guo *et al*. 2010). These observations point to a concomitance between an altered metabolism and w-CIN in a subset of thyroid cancer cells.

Here, we hypothesized that increased levels of reactive oxygen species (ROS) underlie the process of w-CIN in thyroid tumors with NHG. We used DNA content analysis and SNP array technology to search for an NHG in thyroid cancer cell lines in order to investigate the underlying processes. We identified XTC.UC1 cells, the only known cell line model for FTC-OV, and the follicular thyroid cancer cell lines FTC-133, FTC-236 and FTC-238 as models for NHG. Next, we studied the response to metabolic stress and determined the role of ROS and CHK2 activation in whole-chromosome segregation errors by pharmacologic intervention using high-resolution immunofluorescence microscopy as a read-out system in NHG (XTC.UC1, FTC-236) and non-NHG (BHP 2–7, SW579) thyroid cancer cell lines. Finally, we verified our *in vitro* findings in clinical samples and searched for the sequence of whole-chromosome gains or losses in the progression of oncocytic thyroid follicular adenoma to carcinoma.

Methods

Patient material

Selection of cases: SNP array and flow cytometric DNA content data were collected from a cohort of 88 recurrent NMTC cases. Of these, 33 cases showed oncocytic histology by routine H&E histology, determined by an experienced pathologist (HM). Of these, 25 cases showed clear marks of w-CIN (range 1–21 whole-autosomes). One sample was a PTC-OV with the loss of entire chromosome 22. The remaining 24 cases all showed a follicular phenotype and were used to construct a model for the sequential loss of whole chromosomes: 7 oncocytic follicular thyroid adenomas (FA-OV), 1 minimal-invasive oncocytic thyroid follicular carcinoma (FTC-OV-MI), 14 more advanced FTC-OV and 2 anaplastic thyroid carcinomas (ATC) that derived from FTC-OV were included in this study (data submitted to Gene Expression Omnibus, https://www.ncbi.nlm.nih.gov/geo). Morphological evaluation (H&E sections) was performed on the primary tumors without exception. From three patients (Study Nos. 8, 17 and 21), only a metastasis was available for further analysis. From all other patients, primary tumor material was used. Additional patient information on gender, age of diagnosis, invasiveness, recurrence and death of disease can be found in Supplementary Table 1, see section on supplementary data given at the end of this article.

From one patient (No. 15), both formalin-fixed, paraffin-embedded (FFPE) tissue and frozen tissue were available. The oncocytic phenotype showed to be highly associated with whole-chromosomal aberrations ($P<0.0001$, Fisher's exact, two-sided). H&E sections from representative adenoma and cancer cases (Nos. 1, 3, 5, 7, 8, 18 and 23) were scanned with a high-resolution imager (40× magnification, 0.25 µm/pixel, Philips Ultra Fast Scanner 1.6 RA, Philips). Sections (2× and 40× digital zoom) are shown in Supplementary Fig. 1A (Nos. 1, 3, 5 and 7) and B (Nos. 8, 18 and 23).

From the 55 non-oncocytic cases, 6 showed w-CIN (range 1–12 whole-autosomes) and 49 cases showed structural/segmental chromosomal instability (s-CIN, samples show segmental chromosomal defects: chromosomal arms or segments are lost or amplified), a combination of s-CIN and w-CIN or no chromosomal aberrations. One FTC-OV showed s-CIN only. All samples are summarized in Table 1. Samples were handled according to the medical ethical guidelines as described in the Code Proper Secondary Use of Human Tissue (Dutch Federation of Medical Sciences, www.federa.org).

http://erc.endocrinology-journals.org
https://doi.org/10.1530/ERC-17-0288

Table 1 Overview of structural and/or whole-chromosome aberrations found in 88 NMTC cases.

	Chromosomal aberration non-oncocytic				Chromosomal aberration oncocytic variant (OV)			
Histology	s-CIN	w-CIN	s/w-CIN	NC	s-CIN	w-CIN	s/w-CIN	NC
FA				2	1	7**		
FTC-MI					1	1		1
FTC	4	1	3		1	14*		
FVPTC	1	1	2	1				
PTC	11	2	5	14	1	1	1	2
ATC		2	3	3		2*		
Total	16	6	13	20	4	25	1	3

*Samples with an NHG with loss of chromosomes 1–4, 6 and 11 as a minimum genomic signature of FTC-OV; **1/7 FA showed an NHG.
ATC, anaplastic thyroid carcinoma; FA, follicular adenoma; FTC, follicular thyroid carcinoma; FTC-MI, follicular thyroid carcinoma, minimal invasive; FVPTC, follicular variant papillary thyroid carcinoma; NC, no changes observed after LAIR analysis; PTC, papillary thyroid carcinoma; s-CIN, structural chromosomal instability; s/w-CIN, combination of s-CIN and w-CIN; w-CIN, structural chromosomal instability.

Cell lines

The following cell lines were used: BHP 2–7 (derived from a primary papillary thyroid cancer) (Ohta *et al*. 1997), FTC-133, FTC-236, FTC-238 (derived from three different metastases of an FTC) (Demeure *et al*. 1992, Goretzki *et al*. 1990), SW579 (deposited by A Leibovitz) and TT2609-C02 (Geldof *et al*. 2001), all derived from an FTC and XTC.UC1, the only official model for FTC-OV (Zielke *et al*. 1998). All cell lines were cultured under standard conditions (37°C, 5% CO_2 and 95% humidified air). Media were supplemented with glutamine, 10% heat-inactivated FSC and 50 U/mL penicillin and 50 µg/mL streptomycin. FTC-133, FTC-236, FTC-238 and XTC.UC1 were cultured in DMEM-F12. SW579 and TT2609-C02 were maintained in RPMI medium. HeLa cells were taken along as control in metabolic testing. A short tandem-repeat multiplex PCR (Cell ID GenePrint 10 system, Promega) authenticated the cell lines which were no longer cultured than 20 passages and were mycoplasma tested biweekly (in-house PCR method). From FTC-236, seven subclones were generated by limiting dilution: clones A–C, E and G–I. These subclones were maintained in complete DMEM-F12 medium and are available in our laboratory.

DNA content analysis by flow cytometry

For DNA content analysis on cell lines, the Vindeløv method was used (Vindelov *et al*. 1983). In short, cells were harvested by trypsin/EDTA (Corver *et al*. 1995), counted and 2×10^6 cells were divided over two polystyrene tubes. Cells were pelleted and to one tube, trout red blood cells (TRBC) were added as internal reference for DNA content. Next, solutions A, B and C, containing propidium iodide (PI), were added sequentially as described by the method. Samples were stored at 4°C and analyzed next day.

For DNA content of clinical samples, our in-house-developed multiparameter method was used (Corver *et al*. 2005). An LSRII flow cytometer (BD Biosciences, San Jose, CA, USA) was used for collecting FITC, APC and/or PI fluorescence using a 530/30-, 670/14- and 610/20-nm band pass filter, respectively. 488-nm and 635-nm laser lines were used for excitation. Data were analyzed using WinList 8 and ModFit 4 (Verity Software House, Topsham, ME, USA).

DNA isolation

For SNP array analysis (iCOG and HumanCytoSNP-12, Illumina, Inc., San Diego, CA, USA) and mtDNA mutation analysis, high-molecular weight DNA was extracted from frozen samples or frozen cell lines pellets, respectively.

For SNP array analysis of FFPE tissues (GoldenGate assay, Illumina), three 0.6-mm diameter tissue punches (Beecher Instruments, USA) were taken from selected tumor areas (HM) in order to enrich for tumor DNA. Next, tissue punches were dewaxed prior to DNA isolation, and overnight digested with proteinase K at 56°C.

DNA from frozen and FFPE samples was extracted using the NucleoSpin purification kit (Macherey-Nagel GmbH & Co. KG, Düren, BRD, Germany) according to the manufacturer's instructions. DNA concentrations were determined using the Picogreen method (Thermo Fisher Scientific).

Genome-wide SNP array analysis

HumanCytoSNP-12 BeadChip incorporates over 220,000 SNPs across the genome. The ICOG arrays are custom Illumina iSelect genotyping arrays that comprise over 200,000 SNPs. The two high-density platforms were evaluated in-house and showed similar results.

http://erc.endocrinology-journals.org
https://doi.org/10.1530/ERC-17-0288

Arrays were run by a genomics service provider (ServiceXS, Leiden, Netherlands) and hybridized according to the manufacturers' recommendations. The arrays were analyzed as described previously (Corver *et al.* 2008), using the beadarraySNP package (Oosting *et al.* 2007). The GoldenGate is a low-density platform but suitable for fragmented DNA from FFPE tissues. During analysis, the DNA index was incorporated allowing reliable copy number estimates. The method is referred to as Lesser-allele intensity-ratio (LAIR) analysis (Corver *et al.* 2008).

mtDNA sequencing of cell line DNA

Sanger sequencing of mtDNA was performed as extensively described previously (Corver *et al.* 2014). In short, 24 primer pairs (Eurofins MWG Operon, Ebersberg, Germany) were used covering the entire mitochondria and blasted against the National Centre for Biotechnology Information mitochondrial reference genome NC_012920 giving a 100% match. M13 tails were added to the primers for universal sequencing. Purified PCR products were Sanger-sequenced in both directions at MacroGen (Amsterdam, Netherlands). Data were analyzed using Mutation Surveyor version 4.0.8 (MS) (Softgenetics, State College, PA, USA). Variants were called against a GenBank reference (NC_012920) and checked manually. Next, coding missense mutations were selected and analyzed *in silico* using the Polyphen V2 package (Adzhubei *et al.* 2013).

Inhibitors and small molecules

Chemicals and small molecules used: carbonyl cyanide-4-(trifluoromethoxy)phenylhydrazone (FCCP) (Cayman Chemical Company), range 0.5–2.0 µM (stock 30 mM in 100% dimethylsulfoxide (DMSO)); Buthionine sulfoximine (BSO), range 0.01–10 mM ((stock solution 200 mM in Hanks balanced salt solution (HBSS)) (Cayman Chemical), Glutathione (Sigma) 2.0 mM and 20 mM (stock solution 300 in HBSS); N-acetyl cysteine (NAC) (Sigma), 5–30 mM (stock solution 500 mM in HBSS); antimycin A (Cayman Chemical) 2.0 µM (stock solution 10 mM in DMSO); hydrogen peroxide (H_2O_2) (Sigma), 400 µM, diluted in HBSS before use.

Antibodies and fluorescent ROS probe

Primary antibodies: anti-vimentin, clone V9-2b, 1:50 (IgG2b, Cat No. ARA27, Antibodies for Research Applications, BV, Gouda, Netherlands), anti-keratin, clone MNF116, 1:50 (mouse IgG1, Cat No. M0812, Agilent), anti-keratin, clone AE1/AE3, 1:200 (mouse IgG1, Cat No. MA5-13156 (Thermo Fisher Scientific), anti-tubulin, clone DM1A, 1:2000 (ICC), 1:10,000 (blotting) (mouse IgG1, Cat. No. T9026, Sigma-Aldrich), anti-HEC1, clone 9G3, 1:1000 (mouse IgG2a, Cat. No. ab3613, Abcam), anti-pCHK2 (Thr68) (rabbit IgG, Cat. No. 2197, Cell Signaling Technology).

Secondary reagents: goat anti-mouse IgG1-AF488 (Cat. No. A-21121 (Thermo Fisher Scientific), goat anti-mouse IgG2a-AF594 (Cat. No. A-21135, Thermo Fisher), goat anti-rabbit IgG-AF647 (Cat. No. A-21246, (Thermo Fisher Scientific) all diluted 1:200. GaRIgG-IRDye 800CW 1:10,000 and GaMIgG-IRDye 680RD 10,000 (Cat. Nos.: 925-32211 and 925-68070, respectively, LI-COR Biosciences, Lincoln, NE, USA). MitoSOX Red (Cat. No. M36008 Thermo Fisher Scientific), stock 2.5 mM in DMSO, used at 2.5 µM.

Immunofluorescence and imaging

Cells were cultured on alcohol-sterilized APES-coated glass slides (Thermo Fisher Scientific) or in 96-well µClear plates (Cat. No. 655090, Greiner Bio-One International GmbH, Austria), fixed with 4% phosphate-buffered paraformaldehyde (PFA) at 37°C and permeabilized with 100% ice-cold methanol and/or PBS/1%BSA/0.5% Tween20, also used as a blocking step. Staining: α-tubulin and HEC1 followed by a mixture of goat anti-mouse IgG1-AF488 or IgG2A-AF594 supplemented with 0.5 µM Hoechst33342 (Sigma).

Oxygen anion (O_2^-) detection: cells were treated with 2 µM antimycin A for 30 min or left untreated, washed and incubated for 15 min with MitoSox red (Cat. No. M36008, Thermo Fisher Scientific). Next, cells were permeabilized with PBS/1%BSA/0.5% Tween20 after fixation (4% PFA), and indirectly stained for pCHK2 (1:200) and DNA (Hoechst33342, 0.5 µM). Cells were studied using a DM6B fluorescence microscope (Leica). Images were acquired using a CoolPix camera and a 40× immersion oil objective (glass slides) or 40× dry objective (µClear plates).

Immunoblotting

Odyssey nitrocellulose membranes (LI-COR Biosciences) were washed and blocked in TBS Odyssey Blocking Buffer (LI-COR Biosciences) and incubated with an anti-p-CHK2-Thr68/anti α-tubulin mixture. A secondary mixture (GaRIgG-800CW and GaMIgG-680RD) was used for 30 min

http://erc.endocrinology-journals.org
https://doi.org/10.1530/ERC-17-0288

at room temperature. Protein bands were visualized using the Odyssey Classic scanning system.

Oxygen consumption and glycolysis

Twenty thousand cells of each cell line were plated in triplicate in a Seahorse XF^{e}96 microwell plate and cultured overnight. TT2609-C02 did not attach well to the polystyrene and was left out. The cervical carcinoma cell line HeLa was included as a reference (Lee *et al.* 2015). Cells were challenged with different concentrations (0.5–2.0 µM, with steps of 0.5 µM) of FCCP according to the manufacturer instructions or left untreated. Oxygen consumption rates (OCR) and extracellular acidification rates (ECAR) were determined using a Seahorse XF-96 extracellular flux analyzer (Agilent). The OCR and ECAR data were combined into an energy profile.

Statistical analysis

Statistics for lagging, bridged or acentric chromosomes were calculated with a two-tailed Fisher's exact test using Prism 6 software (GraphPad).

Results

w-CIN in thyroid cancer cell lines leads to an NHG

Recently, we proposed a progression model for FTC-OV involving the stepwise loss of entire chromosomes during cancer progression finalizing in an NHG (Corver *et al.* 2012). To find evidence for our hypothesis, we studied seven NMTC cell lines for whole-chromosome losses by the LAIR analysis (Corver *et al.* 2008). XTC.UC1 clearly showed an NHG with most chromosomes in a pure homozygous state ((AA) or (AAA)) (Fig. 1A). The NHG profile in XTC.UC1 was expected, since a CGH copy number profile has been published earlier (Ribeiro *et al.* 2008). FTC-236 (Fig. 1A), FTC-133 and FTC-238 (Supplementary Fig. 2A) also showed an NHG with slightly dissimilar genomic patterns. When cross-referenced at the SNP level, the latter three cell lines are highly related (Supplementary Fig. 2B). Our findings in FTC-133 were similar to the results filed in the COSMIC database (id 906864). Identical to FTC-OV with NHG cell lines, XTC.UC1, FTC-133, FTC-236 and FTC-238 showed homozygous states of chromosomes 1–4, 6 and 11. The average DNA indices of XTC.UC1, FTC-133, FTC-236 and FTC-238 are shown in Table 2. Apparently, identical to cases of FTC-OV with NHG, ancestors of these cells in the primary tumor or during cell line development underwent endoreduplication. Interestingly, in FTC-236, we identified by flow cytometric DNA content analysis two populations implying CIN and selective outgrowth during culture (Fig. 1B). Hence, we performed the LAIR analysis on seven newly established FTC-236 subclones. The obtained results pointed to continuous asymmetric reciprocal mitotic events during *in vitro* culture of FTC-236 cells (Fig. 1C). Subclones FTC-236G and -H showed near-identical NHGs but differed in morphology and chromosome copy numbers as observed by the DNA index (Supplementary Fig. 3). From these observations, we deduced a model of segregation errors of chromosome 18 in FTC-236 (Fig. 1D). Alternatively, the missegregated chromosome may lag behind and forms a micronucleus after mitosis. Indeed, FTC-236 showed approximately 10 times higher numbers of micronuclei than BHP 2–7 under standard culture conditions (Supplementary Fig. 4). The LAIR profiles of BHP 2–7 and SW579 were clearly different and showed s-CIN (BHP 2–7) or a mixture of w-CIN and s-CIN (SW579) (Supplementary Fig. 5). TT2609-C02 was published earlier and also showed a mixture of w-CIN and s-CIN (Boot *et al.* 2016).

Collectively, these *in vitro* findings further support our proposed hypothesis that a subset of follicular thyroid cancers, especially those with oncocytic metaplasia, show sustained missegregations during mitosis with selection pressure on whole-chromosome losses leading to NHG.

FTC cell lines harboring an NHG show a quiescent metabolic phenotype

FTC-OV is tightly associated with an altered metabolism (Mirebeau-Prunier *et al.* 2013). XTC.UC1 is a model for clinical FTC-OV and shows a relative quiescent glycolysis and oxidative metabolism (Lee *et al.* 2015). Since FTC-133, -236 and -238 also harbor an NHG, we questioned whether these cells show a comparable metabolism. The energy profiles of FTC-133, FTC-236 and FTC-238 were highly comparable to the relative quiescent energy profile of XTC.UC1 (Fig. 2A). In contrast, BHP 2-7, SW579 and HeLa showed a higher basic ECAR and OCR and showed a significant increase in ECAR and OCR after exposure to FCCP.

Owing the highly comparable energy profiles, we next questioned whether FTC-133, -236 and -238 also harbor explanatory disruptive mtDNA mutations like XTC.UC1. We sequenced the entire mitochondrial genomes of the seven NMTC cell lines used in this study using twenty-four overlapping fragments (Corver *et al.* 2014). We confirmed the known disruptive C insertion at bp3571, causing a stop

http://erc.endocrinology-journals.org
https://doi.org/10.1530/ERC-17-0288

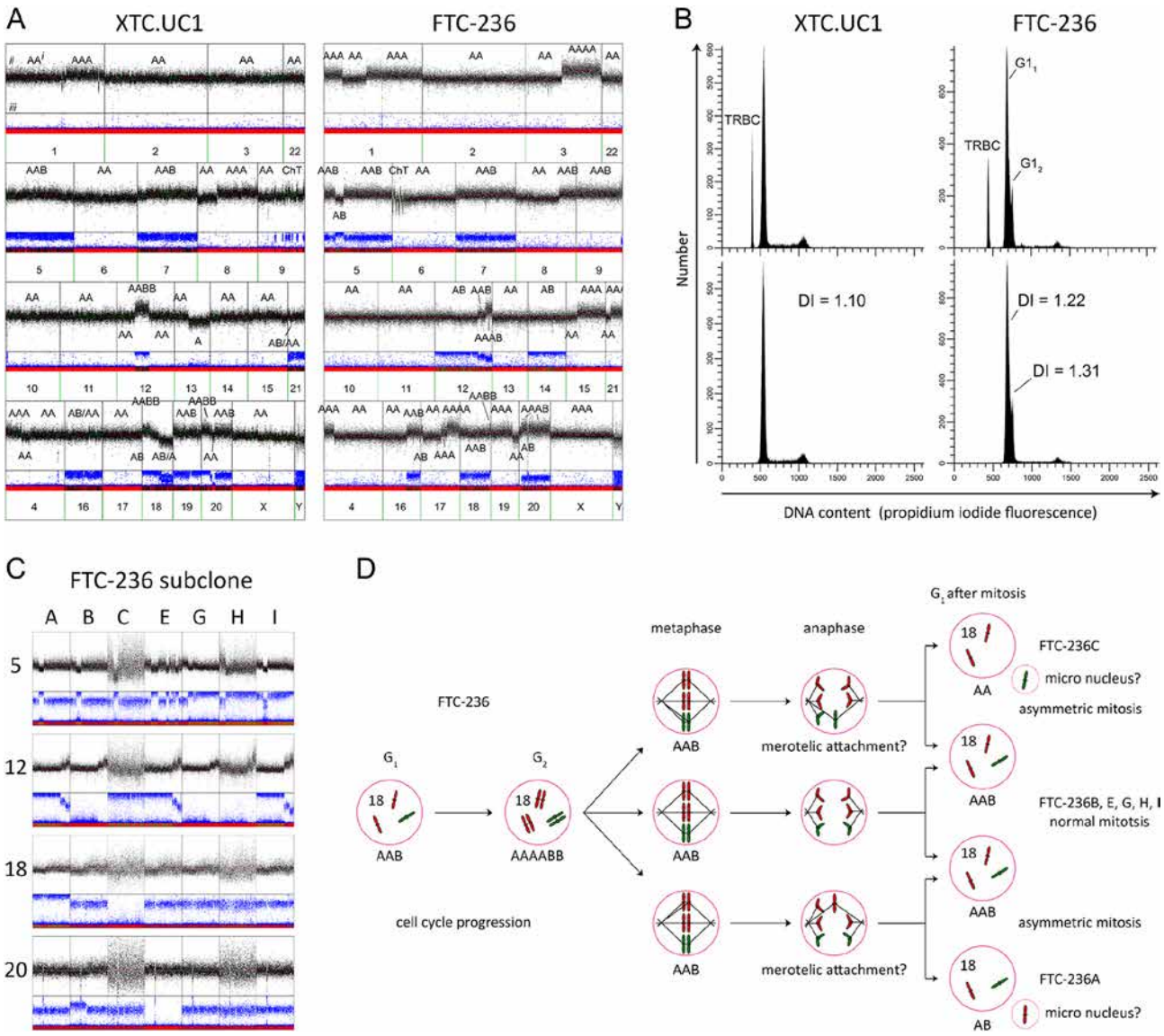

Figure 1
Lesser-allele intensity-ratio analysis (LAIR) of XTC.UC1, FTC-236 follicular thyroid cancer cells and FTC-236 subclones shows whole-chromosome missegregations. (A) LAIR analysis of XTC.UC1 and FTC-236. Note that many autosomes (1–4, 6, 8, 10, 11, 13, 15 and 17) showed a homozygous state (AA), highly comparable to clinical FTC-OV samples after endoreduplication of the entire near-haploid genome. (B) Flow cytometric DNA content analysis of, respectively, the oncocytic follicular thyroid cancer cell line XTC.UC1 (left panels) and the follicular thyroid cancer cell line FTC-236 (right panels). Two cycling populations were observed in FTC-236, with a DI of 1.22 and 1.31. (C) Selection of seven FTC-236 subclones after limiting dilution showing subtle intra-subclone chromosomal differences in chromosomes 5, 12, 18 and 20. A reciprocal event was observed for chromosome 18: compare clone A (AB), clones B, E, G, H and I (AAB) and clone C (A). (D) A model is proposed for asymmetric mitotic events in FTC-236, possibly caused by merotelic-attached kinetochores or excessive stability of the kinetochore–microtubule attachment. *i*, allelic state; *ii*, copy number; *iii*, 0<allelic ratio<1; (AB) or (AABB), heterozygous; (AAB) or (AAAB), imbalance; (AA) or (AAA), etc., homozygous; ChT, chromotripsis; TRBC, trout red blood cells; DI, DNA index; $G1_1$, G1 of the major cycling population; $G1_2$, G1 of the minor cycling population.

codon at amino acid 101 (*MT-ND1*, subunit of complex I) and the damaging mutation (m.15557 G>A: p.271E>K) in *MT-CYB* (complex III) (Bonora *et al*. 2006) in XTC. UC1. No further disruptive mutations were found in the remaining cell lines. Only damaging mtDNA mutations and silent polymorphisms were observed (Fig. 2B and Table 2). This supports our earlier observation in clinical samples that mtDNA mutations neither associate with an NHG nor with a relative quiescent energy profile (Corver *et al*. 2014).

In conclusion, a modified relatively quiescent metabolic phenotype might be linked to the establishment

http://erc.endocrinology-journals.org
https://doi.org/10.1530/ERC-17-0288

Table 2 Cell line characteristics.

						Mitochondrial DNA mutations			
Cell line	**Gender**	**Age**	**Localization**	**Origin**	**NHG**	**DI**	**Complex**	**MT-gene**	**Mutation**	**PolyPhen-2 (HumVar)**
BHP 2–7	f	u.k.	Primary	PTC	N	1.07	–	variants	–	–
FTC-133	m	42	Lymph node	FTC	Y	1.35	I	*ND6*	m.14198 G>A: p.159T>I	0.884
FTC-236	m	42	Neck lymph node	FTC	Y	1.22	I	*ND6*	m.14198 G>A: p.159T>I	0.884
FTC-238	m	42	Lung	FTC	Y	1.19	I	*ND6*	m.14198 G>A: p.159T>I	0.884
SW579	m	59	Primary	FTC	N	1.58	I	*ND5*	m.12634 A>G: p.100I>V	0.943
TT2609-C02	m	57	Primary	FTC	N	1.55	I/IV	*ND5/COX1*	m.13415 G>A: p.360 G>E/m.6063 T>C: p.54Y>H	1.0/0.965
XTC.UC1	f	63	Soft tissue breast	FTC-OV	Y	1.10	I/III	*ND1/CYTB*	m.3571dupC/m.15557 G>A: p.271E>K	Stop at p.101/0.998

DI, DNA index; FTC, follicular thyroid cancer; FTC-OV, follicular thyroid cancer of the oncocytic variant; MT-gene, mitochondrial gene; NHG, near-homozygous genome (Yes or No); PTC, papillary thyroid cancer; u.k., unknown.

of an NHG in FTC-OV. In the tested thyroid cancer cell lines, a relation between the mtDNA status and a certain metabolic phenotype or an NHG is not evident.

ROS is linked to chromosome missegregation errors in FTC-OV

Next, we questioned how an altered metabolism is related to an NHG in the NMTC cell line models FTC-133, -236, - 238 and XTC.UC1. XTC.UC1 is known to generate high levels of ROS (Stankov *et al.* 2006) and complex III, which plays a significant role in regulating ROS (Chen *et al.* 2003), is overexpressed in FTC-OV (Baris *et al.* 2005). Since ROS can activate ATM-CHK2 in a DNA damage-independent manner (Alexander *et al.* 2010, Guo *et al.* 2010) and ATM-CHK2 activation can cause lagging chromosomes (Bakhoum *et al.* 2014), ROS might underlie the development of an NHG.

Under basal conditions, XTC.UC1 cells and FTC-236 cells showed significantly higher numbers of lagging chromosomes than SW579 and BHP 2-7 cells ($P=0.006$), whereas XTC.UC1 and FTC-236 were highly comparable ($P>0.5$). Lagging chromosomes but also chromatin bridges, acentric chromatin or combinations were primarily found in XTC.UC1 and FTC-236 (Fig. 3A). XTC.UC1 showed significantly more chromosome bridges ($P=0.0002$) and acentric chromosomes than BHP 2–7 ($P=0.027$).

We then asked whether we can reduce the number of segregations errors in the latter two cell lines using pharmacological intervention affecting ROS. BHP 2–7 was taken for comparison. NAC is a potent ROS scavenger and serves as a precursor of cysteine for glutathione (GSH) synthesis, an important cellular antioxidant (Samuni *et al.* 2013). Treating the cells with 5–15 mM NAC significantly decreased the number of anaphase missegregations ($P<0.05$) in XTC.UC1 and FTC-236 compared to high basal levels (Fig. 3B).

Next, we questioned whether CHK2 might be involved. Indeed, XTC.UC1 cells, the oncocytic cell line with a high frequency of spontaneous chromosome missegregations, showed phosphorylation CHK2 under standard culture conditions. pCHK2 diminished after glutathione addition in a dose-dependent manner. Treating the cells with H_2O_2 significantly increased the signal amplitude of CHK2 phosphorylation (Fig. 3C). We then induced superoxide anion (O_2^-), the main component of mitochondrial ROS, by inhibiting complex III using antimycin A. A moderate increase in CHK2 phosphorylation was observed (Fig. 3C) exclusively caused by further CHK2 activation in metaphase nuclei (Fig. 3D)

http://erc.endocrinology-journals.org
https://doi.org/10.1530/ERC-17-0288

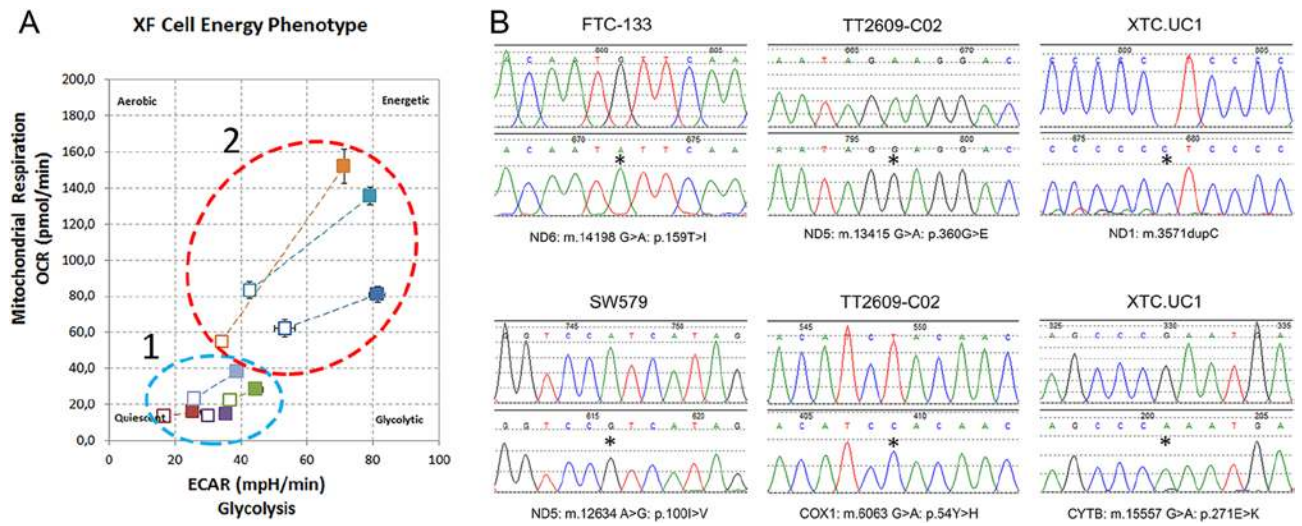

Figure 2

A low-energetic phenotype corresponds to follicular thyroid cancer cell lines with an NHG but not with mtDNA mutations. (A) Energy profiles of FTC-133, -236 and -238, XTC.UC1 (all showing an NHG) vs BHP 2–7, SW579 and HeLa after challenging with FCCP. Abscissa: ECAR, ordinate: OCR. Open squares: ECAR/OCR untreated cells, closed squares ECAR/OCR FCCP treated cells. Note that FTC-133 (dark red), -236 (green) and -238 (purple), XTC.UC1 (gray) show a relative quiescent profile (cluster 1, blue-dotted circle), while BHP 2–7 (dark gray/blue), SW579 (orange) and HeLa (light gray/blue) show a strong increase in both glycolysis and oxygen consumption (cluster 2, red-dotted circle). (B) Damaging/disruptive mtDNA mutations in all thyroid cancer cell lines tested except for BHP 2–7. FTC-133, -236 and -238, derived from different metastasis from the same patient, share the same mutation. The known mutations in XTC.UC1 were confirmed (Table 2). Also note that SW579 shows a relative strong energetic response when challenged with FCCP, despite a damaging mtDNA mutation.

which simultaneously showed an increase in MitoSOX Red fluorescence, an O_2^- indicator (Fig. 3D). Interphase nuclei did not show pCHK2 fluorescence. The same was observed in BHP 2–7 cells but with lower fluorescent signal amplitudes (Supplementary Fig. 6). By treating BHP 2–7 cells with BSO, an inhibitor of γ-glutamylcysteine synthetase, the rate-limiting enzyme for GSH synthesis, the number of missegregations increased significantly and a subtle increase in CHK2 phosphorylation were observed in mitotic cells (Supplementary Fig. 7). This demonstrated that the ATM-CHK2 pathway is active in these cell lines and that O_2^- can regulate the levels of pCHK2. Thus, ROS is likely involved in chromosomal missegregations in XTC.UC1 and in FTC-236 thyroid cancer cells by activating CHK2 signaling.

Whole-chromosome segregation errors underlie the progression toward NHG

To also find evidence for a sustained process of whole-chromosome reciprocal missegregations in (oncocytic) follicular thyroid tumors cases, we compared 7 FA-OV, 15 FTC-OV and 2 ATC both derived from an FTC-OV.

All carcinoma cases and 3 FA-OV in this study showed whole-chromosome losses. Strikingly, two FA-OV and the FTC-OV-MI case presented imbalances of whole chromosomes which showed homozygous in 100% (chromosomes 1 and 2), 94% (chromosomes 8 and 22), 88% (chromosome 9) and 65% (chromosome 18) of the FTC-OV samples ($n=17$) (Fig. 4A), indicating that these losses might be early events in tumor development. Additional losses of chromosomes 2, 3, 6, 11, 14–16 and 21 seem to be associated with tumor progression with losses of chromosomes 1–4, 6 and 11 as minimum signature of FTC-OV. Four FA-OV showed copy number gains only.

From one FTC-OV, we observed differences between two samples (Nos. 15a and 15b). Sample 15a showed heterozygous (AABB) for chromosomes 12, 13 and 18, while sample 15b is homozygous for these chromosomes (AA). This clearly demonstrates intra-tumor heterogeneity which can be the result of a sustained process of w-CIN active in FTC-OV cases. Whole-genome DNA sequencing (Nos. 11, 15a and 23) further confirmed our SNP array findings (Supplementary Fig. 8).

Together, our observations point to an initiating asymmetric mitotic event in which the retention of chromosome 7 (status (AAB) or (AB)), and, to a lesser extent, chromosomes 5 and 12 is crucial and selected during further progression. Apparently, the reciprocal counterparts with chromosomes 5, 7 and/or 12 in a homozygous state (A) do not survive or favor a selective outgrowth, likely driven

http://erc.endocrinology-journals.org
https://doi.org/10.1530/ERC-17-0288

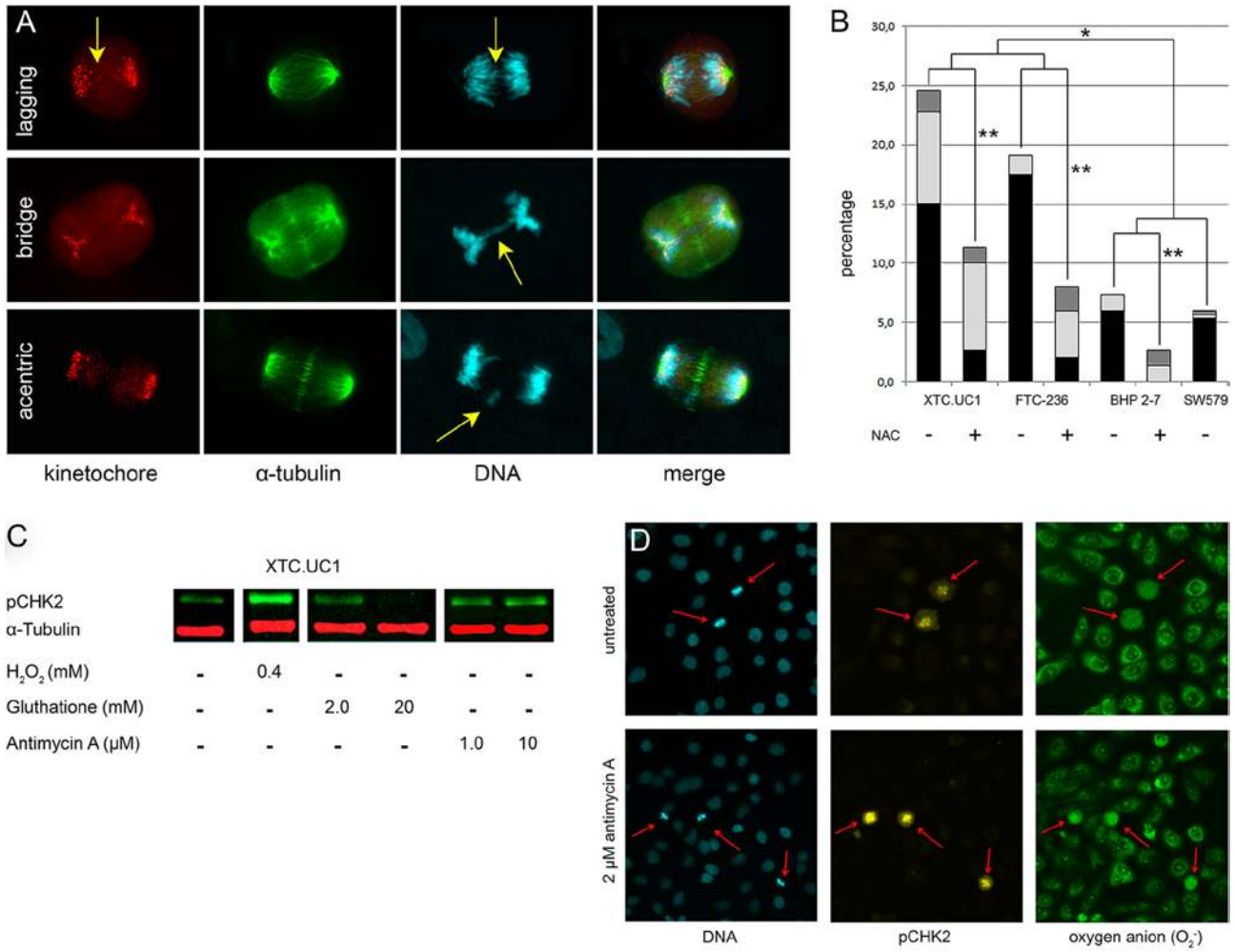

Figure 3
ROS is linked to missegregations via CHK2 activation. (A) Examples of spontaneous missegregations in XTC.UC1 showing: a lagging chromosome (upper row), a chromatin bridge (middle row) and an acentric chromosome (lower row). From left to right: kinetochore (red, AF594 fluorescence), α-tubulin (green, AF488 fluorescence), DNA (cyan, Hoechst33342 fluorescence), merged image. All images were captured with a 40× dry objective. An identical digital zoom was applied to all images. (B) XTC.UC1 and FTC-236 show a significant higher number of lagging chromosomes than BHP 2–7 and SW579 (*P=0.0004) (n=300). Strong reduction (**P<0.0001) of the percentage of mainly lagging chromosomes in XTC.UC1, FTC-236 and BHP 2–7 after treatment the cells for 2 h with the ROS scavenger NAC. Black: lagging chromosomes, gray: chromosome bridge, white: acentric chromosomes. (C) Western blot showing auto-phosphorylation of CHK2 in XTC.UC1 cells (in green), α-tubulin internal control (red). CHK2 can be further activated by H_2O_2, while glutathione treatment reduced the amplitude of phosphorylation. An increase in pCHK2 was shown after incubating the cells with antimycin A. (D) XTC.UC1 cells were treated with antimycin A (lower panels) or left untreated (upper panels) and stained for ROS, pCHK2 and DNA. Increased ROS activity (MitoSOX Red, in green) was observed in many metaphase cells (see red arrows), which coincided with an increased pCHK2 fluorescence (in yellow, AF647 fluorescence). DNA was stained with Hoechst33342 (cyan). All images were captured with a 20× dry objective. An identical digital zoom was applied to all images.

by imprinted genes on chromosome 7 (Boot *et al.* 2016). Genomic ranking further supports our hypothesis of a sustained process of whole-chromosome segregation errors and selection for whole-chromosome losses (Fig. 4B) in the progression from FA-OV to FTC-OV and ATC-derived FTC-OV. Progression by additional chromosomal losses (Study Nos. 13–24, Fig. 4B) seems to be associated with death of disease (Supplementary Table 1).

Discussion

We propose that ROS is linked to the massive loss of whole chromosomes during oncocytic follicular thyroid tumor progression resulting in an NHG. Despite the fact that molecular mechanisms implicated in w-CIN are studied extensively; a common cause leading to near-haploidy in cancer is yet to be identified. Even in the era of

http://erc.endocrinology-journals.org
https://doi.org/10.1530/ERC-17-0288

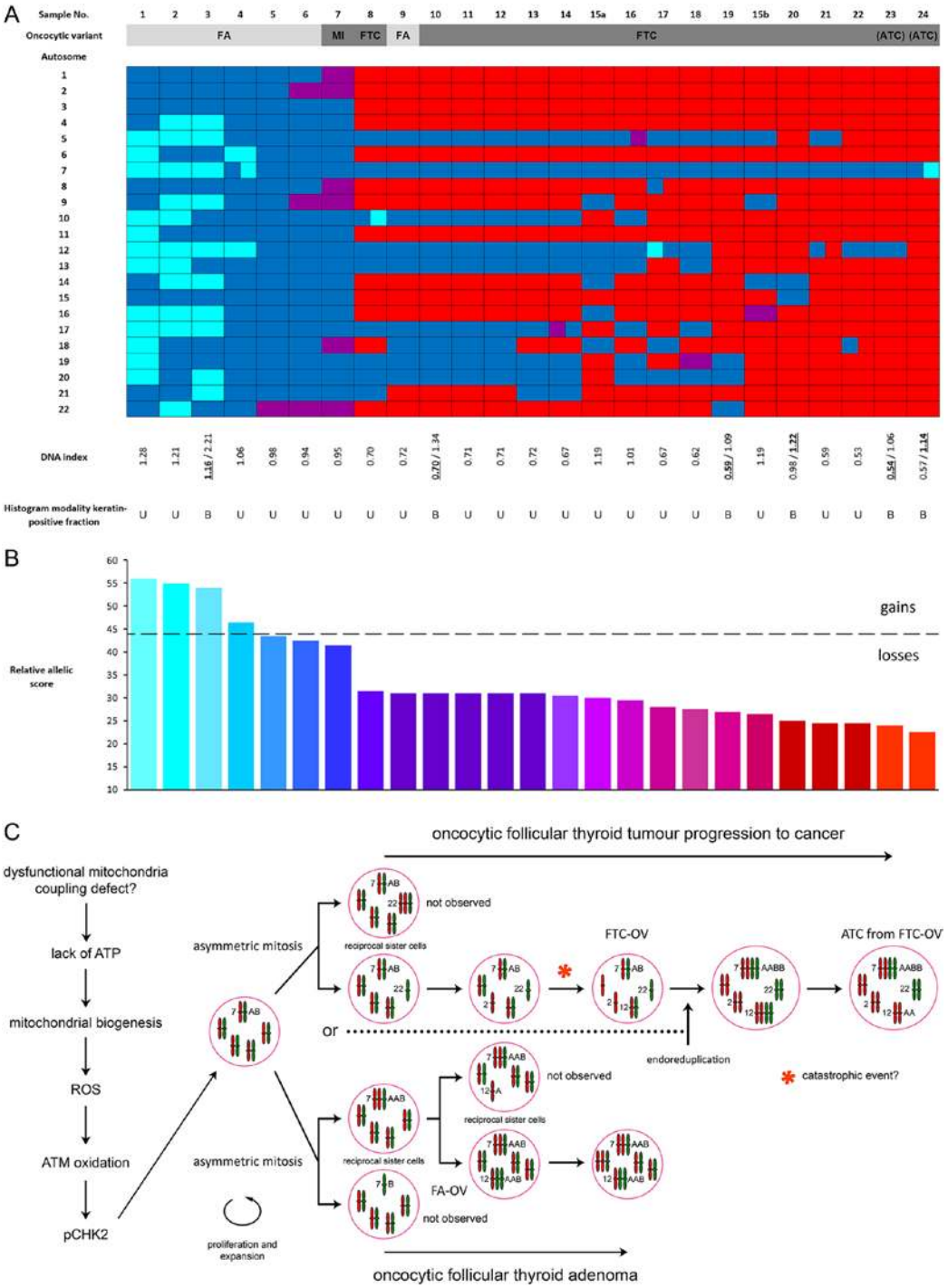

Figure 4

Genomic ranking and proposed tumor progression model for oncocytic follicular thyroid cancer. (A) Ranking of oncocytic follicular thyroid tumors based on whole chromosome losses or gains. The DNA index was obtained by multiparameter flow cytometry of cell suspension derived from FFPE tissue punches. Seven samples were bimodal (B) and samples 3, 10, 15 19, 20, 23 and 24 show endoreduplication (genome doubling). (B) Sum of the relative allelic score showing progressive whole-chromosome losses or gains. Note the relative sharp transition from FA-OV to FTC-OV. (C) Newly proposed model for FTC-OV tumor progression based on the activation of CHK2 via direct ATM oxidation by high ROS. This results in increased tension of the kinetochore/α-tubulin network leading to whole-chromosome segregation errors (Bakhoum *et al.* 2014). The progression from FA-OV seems to be driven by a stepwise loss of whole chromosomes, but with retention of chromosome 7 due to maternal- and paternal-imprinted genes important for survival (Boot *et al.* 2016). The loss of chromosome 22 is an early event. Blue, heterozygous (AB) or (AABB), score 2.0; light blue, imbalance (AAB), score 3.0; purple, imbalance composed of a mixture of status (AB) and (A), score 1.5; red, homozygous (A) or (AA), etc., score 1.0; B, bimodal DNA histogram (underlined: major population); U, unimodal DNA histogram.

http://erc.endocrinology-journals.org
https://doi.org/10.1530/ERC-17-0288

next-generation sequencing (NGS), candidate gene variants directly related to whole-chromosome segregation errors are rarely found. For example, inactivation of the long non-coding RNA NORAD results in chromosome bridges and mitotic slippage, a common route to high aneuploidy (Lee *et al.* 2016). However, chromosome bridges do not explain the whole-chromosome losses found in FTC-OV with NHG. Relative low numbers of chromosomal bridges were found in XTC.UC1 and FTC-236. Moreover, in FTC-OV, gene variants or fusions in cancer driver genes are relatively rare, although those found (e.g. *FLCN*, *MEN1*, *mTOR*, *PTEN*, *PIK3CA*, *TP53* and *TSC2*, Table 3) are frequently involved in metabolic switches. Possibly additional tumor drivers need to be identified. Indeed, we only found a *PTEN*- and a *TP53*-inactivating gene variant after whole-genome sequencing (WGS) of three FTC-OV with NHG (data not shown). Thus, FTC-OV does not seem to share the same mutation(s) or share the same mutated gene(s) which can be directly related to w-CIN.

Alternatively, we now suggest that the ubiquitous loss of whole chromosomes in FTC-OV with NHG might be a tumor driver induced by oxidative stress. ROS are the main mitochondrial side products. As mentioned earlier, ROS can activate CHK2 in a DNA damage-independent manner (Alexander *et al.* 2010, Guo *et al.* 2010), while CHK2 activation during mitosis induces chromosome segregation errors (Bakhoum *et al.* 2014).

By pharmacological intervention using the antioxidant NAC, we were able to significantly reduce the ongoing process of chromosome missegregations in XTC.UC1 and FTC-236 cells, models for NHG-associated oncocytic – and follicular thyroid cancer. The missegregations are probably driven by CHK2 since glutathione treatment diminished CHK2 autophosphorylation.

Our work also implies that the process of whole-chromosome segregation errors is on-going in clinical FTC-OV, demonstrated by intra-tumor heterogeneity (samples 15a and 15b) and the progressive loss of whole chromosomes toward subsets of ATC that is derived from FTC-OV (samples 23 and 24) with only chromosomes 7 and 12, and 7 in a heterozygous state, respectively. The latter observation was confirmed by others in a particular case of an ATC with responsiveness to everolimus (Wagle *et al.* 2014). Furthermore, progressive loss of whole chromosomes seems to be associated with a poor prognosis. Especially, the thyroid cancer patients with extensive whole-chromosome losses (twelve out of seventeen) died of disease (Supplementary Table 1), though this must be confirmed in a larger cohort. Using FTC-236 as an *in vitro* model, we showed that sister chromatids can be asymmetrically distributed over the two sister cells after a reciprocal mitotic event and that both sister cells are viable as demonstrated by the outgrowth of these clones. However, genomically reciprocal tumors were not observed in our cohort of clinical samples. Markedly, chromosomes 1–4, 6 and 11, which mainly comprises the larger chromosomes, were preferentially lost in FTC-OV, whereas overall in human carcinomas, the smaller chromosomes are lost (Duijf *et al.* 2013). As mitosis is an energy-demanding process and FTC-OV show an impaired ATP synthesis (Bonora *et al.* 2006, Savagner *et al.* 2001), it might be beneficial to lose larger chromosomes early in the progression process in order to save energy during mitosis. However, as we showed before in oncocytic adrenocortical cancer and in oncocytic follicular thyroid cancer, disruptive mtDNA mutations, which might underlie a lack of ATP, do not solely explain the phenomenon of NHG (Corver *et al.* 2014). Disruptive mtDNA variations were also not found in the NHG cell lines FTC-133, -236 and -238. Together with the lack of a uniform nuclear gene variant in oncocytic tumors, the proliferation of mitochondria seen in both oncocytic follicular adenomas and carcinomas might partly be stress-related, possibly caused by a coupling defect (Savagner *et al.* 2001).

Hence, there seems to be a strong selection pressure on whole-chromosome losses after a pivotal asymmetric or reciprocal mitotic event in the development of FTC-OV, respectively. Other, probably random, whole-chromosome asymmetric mitotic events do not have a growth advantage or cells involved undergo apoptosis. Based on our observations, we propose a new progression model for (oncocytic) follicular thyroid tumors toward NHG with ROS and CHK2 activation as drivers of the process (Fig. 4C). The latter is characterized by a stepwise loss of whole chromosomes toward an NHG and cancer in which chromosome 22 might be a marker of progression.

Our data seem partly conflicting with earlier studies which demonstrated chromosomal copy number gains rather than losses in FTC-OV in most studies. Actually, previous findings are not that dissimilar from ours but were differently interpreted. We combined SNP array and multiparameter flow cytometric DNA content analyses, which provides allele-specific information and accurate copy numbers (Corver *et al.* 2008). The latter approach demonstrated that FTC-OV are dominated by whole-chromosome losses during tumor progression and that approximately 44% (Fig. 4A) of the cases in our cohort showed endoreduplication (genome doubling) of their entire NHG genome. For example, two copies of chromosomes

http://erc.endocrinology-journals.org
https://doi.org/10.1530/ERC-17-0288

Table 3 A variety of genes mutated in FA-OV or FTC-OV cases (Hürthle cell carcinomas).

Mutation/rearrangement fusions	Number of cases	Histology	Technique	% Positive	Reference
STK11, TP53***	1	FTC-OV (with clear-cell features)	NGS (targeted)	100 (1/1)*,**	Wei *et al.* (2016)
KRAS, HOOK3**, no fusions*	6 6	FA-OV FTC-OV	RNA-seq	17 (1/6)* 17 (1/6)**	Pagan *et al.* (2016)
BRAF	1	FTC-OV[$]	PCR (BRAF)	100 (1/1)	Sinno *et al.* (2016)
PTEN, TP53***	12	FTC-OV	NGS (targeted)	25 (3/12)* 42 (5/12)**	Wei *et al.* (2015)
TERT, BRAF***	3	FTC-OV	PCR + direct sequencing	67 (1/3)* 0 (0/3)**	Qasem *et al.* (2015)
TERT	48 13	FTC-OV FTC-OV (MI)	qPCR	13 (6/48) 15 (2/13)	Chindris *et al.* (2015)
TP53, BRAF**, (HRAS, KRAS, NRAS)***, PAX8/PPARγ****, RET/PTC******	45	FTC-OV	PCR (TP53, BRAF, HRAS, KRAS, NRAS) RT-PCR (PAX8/PPARγ)FISH (RET/PTC)	6.6 (3/45)* 4.4 (2/45)** 6.6 (3/45)*** 50 (5/10)**** 3.8 (1/26)*****	Evangelisti *et al.* (2015)
MEN1 (EWSR1**, BRCA1***, MSH2***)*	2	FTC-OV (fresh/frozen)* shared in both tumors, **primary tumor, ***metastasis of the same tumor	Whole-genome sequencing Sanger sequencing for verification	100 (2/2)	Kasaian *et al.* (2015)
TSC2, TP53*, FLCN*, mTOR***	1 1	ATC (from FTC-OV)	Whole-exome sequencing	100 (1/1)* primary tumor 100 (1/1)*,** only in the post-resistance biopsy	Wagle *et al.* (2014)
HRAS, NRAS, PAX8/PPARγ, RET/PTC	12	FTC-OV	RT-PCR	0 (0/12)	Mond *et al.* (2014)
*BRAF, HRAS, KRAS, NRAS**	12 7	FA-OV FTC-OV	PCR	8.3 (1/12)* 0 (0/7)	Schulten *et al.* (2013)
TERT	17 8	FTC-OV FTC-OV (MI)	PCR	24 (4/17) 0 (0/8)	Landa *et al.* (2013)
BRAF, HRAS, KRAS, NRAS, PIK3CA, PAX8/PPARγ, RET/PTC, NTRK1, AKAP9-BRAF* rearrangement	8 19	FA-OV FTC-OV	Mass spectometry genotyping (targeted) RT-PCR (rearrangements)	0 (0/8) 0 (0/8), no rearrangements 16 (3/19)* 0 (0/19), no rearrangements	Ganly *et al.* (2013)
PAX8/PPARγ, RET/PTC**, BRAF, HRAS, NRAS****	3 17	FA-OV FTC-OV	FISH PCR	33 (1/3)* 27 (4/17)** 38 (6/17)** 5.8 (1/17)*,** 5.8 (1/17)***	de Vries *et al.* (2012)
*EGFR, HRAS, KRAS, NRAS, PIK3CA**	15	FTC-OV	PCR (Sanger)	6.7 (1/15)*	Corver *et al.* (2012)
EGFR	1	FTC-OV (focally anaplastic)	PCR (followed by sequencing)	100 (1/1)	Hogan *et al.* (2009)
BRAF	21 20	FA-OV FTC-OV	PCR (followed by direct sequencing)	0 (0/21) 0 (0/20)	Musholt *et al.* (2008)
BRAF, NRAS, PAX8/PPARγ1	9	FTC-OV	PCR (followed by direct sequencing)	0 (0/9)	Di Cristofaro *et al.* (2006)
GRIM-19	20 6	FTC-OV FTC-OV (familial)	PCR (followed by direct sequencing)	15 (3/20) 0 (0/6)	Maximo *et al.* (2005)
HRAS, KRAS, NRAS*	7 4	FA-OV FTC-OV	PCR (followed by SSCP)	0 (0/7) 25 (1/4)*	Tallini *et al.* (1999)
TSHR	1	FTC-OV	PCR (followed by SSCP)	0 (0/1)	Spambalg *et al.* (1996)

A survey of the known literature on oncocytic adenoma and carcinoma was carried out. A plethora of techniques has been used and various mutations and/or rearrangements have been found by many different research groups. * or ** or ***, etc. corresponds to the percentage (x) and number of positive samples (y) of the total number of samples tested (z) in x(y,z) for a certain mutation/rearrangement/fusion in each study.
FISH, fluorescence *in situ* hybridization; NGS, next-generation sequencing; PCR, polymerase chain reaction; qPCR, quantitative polymerase chain reaction; RNA-seq, RNA sequencing; RT-PCR, reverse transcriptase polymerase chain reaction; SSCP, single-strand conformational polymorphism.

http://erc.endocrinology-journals.org
https://doi.org/10.1530/ERC-17-0288

7 and 12 in a heterozygous state (AB) in a near-haploid (A) genomic background will be interpreted as gains by array-CGH. After endoreduplication also, the homozygous state of the residual chromosomes (AA) will not be seen by FISH.

Our observations regarding NHG in thyroid tumors have recently been confirmed (Kasaian *et al*. 2015) and have so far exclusively been found in NMTC with an oncocytic follicular histology or ATC that progressed from an FTC-OV (Wagle *et al*. 2014). However, the thyroid cancer cell lines FTC-133, -236 and -238 showed NHG but were reported to be derived from non-oncocytic FTC.

We now conclude that CHK2 activation via ROS is a dominant driver in the carcinogenesis of FTC-OV lesions with NHG, although we cannot rule out that the same or a comparable mechanism is active in the progression of other subsets of thyroid tumors.

Supplementary data

This is linked to the online version of the paper at https://doi.org/10.1530/ERC-17-0288.

Declaration of interest

The authors declare that there is no conflict of interest that could be perceived as prejudicing the impartiality of the research reported.

Funding

This work was partially supported by the Dutch Cancer Society (Koningin, Wilhelmina Fonds, KWF) UL 2010-4656 (T van Wezel and H Morreau).

Authors' contribution statement

Conception and design: W E Corver, H Morreau. Pathology: H Morreau. Acquisition of data: W E Corver, S Sahraeian, J Demmers, T van Wezel, A Boot. Analysis and interpretation of data (e.g., computational analysis, statistical analysis, biostatistics): W E Corver, D Ruano Neto, J Oosting. Reviewing manuscript: all authors Writing and revision of the manuscript: W E Corver, H Morreau.

Acknowledgements

XTC.UC1 (oncocytic follicular thyroid carcinoma, passage number p122) was kindly provided by Dr Orlo Clark, UCSF. The authors want to thank Dr Joop Wiegant (LUMC) and Dr Theo Plantinga (NUMC) for supporting them with fluorescence microscopy and WGS analysis, respectively.

References

Adzhubei I, Jordan DM & Sunyaev SR 2013 Predicting functional effect of human missense mutations using PolyPhen-2. *Current Protocols in Human Genetics* **Chapter 7** Unit 7. (https://doi.org/10.1002/0471142905.hg0720s76)

Alexander A, Cai SL, Kim J, Nanez A, Sahin M, MacLean KH, Inoki K, Guan KL, Shen J, Person MD, *et al*. 2010 ATM signals to TSC2 in the cytoplasm to regulate mTORC1 in response to ROS. *PNAS* **107** 4153–4158. (https://doi.org/10.1073/pnas.0913860107)

Bakhoum SF, Kabeche L, Murnane JP, Zaki BI & Compton DA 2014 DNA-damage response during mitosis induces whole-chromosome missegregation. *Cancer Discovery* **4** 1281–1289. (https://doi.org/10.1158/2159-8290.CD-14-0403)

Baris O, Mirebeau-Prunier D, Savagner F, Rodien P, Ballester B, Loriod B, Granjeaud S, Guyetant S, Franc B, Houlgatte R, *et al*. 2005 Gene profiling reveals specific oncogenic mechanisms and signaling pathways in oncocytic and papillary thyroid carcinoma. *Oncogene* **24** 4155–4161. (https://doi.org/10.1038/sj.onc.1208578)

Bonora E, Porcelli AM, Gasparre G, Biondi A, Ghelli A, Carelli V, Baracca A, Tallini G, Martinuzzi A, Lenaz G, *et al*. 2006 Defective oxidative phosphorylation in thyroid oncocytic carcinoma is associated with pathogenic mitochondrial DNA mutations affecting complexes I and III. *Cancer Research* **66** 6087–6096. (https://doi.org/10.1158/0008-5472.CAN-06-0171)

Boot A, Oosting J, de Miranda NF, Zhang Y, Corver WE, van de Water B, Morreau H & van Wezel T 2016 Imprinted survival genes preclude loss of heterozygosity of chromosome 7 in cancer cells. *Journal of Pathology* **240** 72–83. (https://doi.org/10.1002/path.4756)

Chatterjee A, Mambo E & Sidransky D 2006 Mitochondrial DNA mutations in human cancer. *Oncogene* **25** 4663–4674. (https://doi.org/10.1038/sj.onc.1209604)

Chen Q, Vazquez EJ, Moghaddas S, Hoppel CL & Lesnefsky EJ 2003 Production of reactive oxygen species by mitochondria: central role of complex III. *Journal of Biological Chemistry* **278** 36027–36031. (https://doi.org/10.1074/jbc.M304854200)

Chindris AM, Casler JD, Bernet VJ, Rivera M, Thomas C, Kachergus JM, Necela BM, Hay ID, Westphal SA, Grant CS, *et al*. 2015 Clinical and molecular features of Hurthle cell carcinoma of the thyroid. *Journal of Clinical Endocrinology and Metabolism* **100** 55–62. (https://doi.org/10.1210/jc.2014-1634)

Corver WE, Cornelisse CJ, Hermans J & Fleuren GJ 1995 Limited loss of nine tumor-associated surface antigenic determinants after tryptic cell dissociation. *Cytometry* **19** 267–272. (https://doi.org/10.1002/cyto.990190311)

Corver WE, Ter Haar NT, Dreef EJ, Miranda NF, Prins FA, Jordanova ES, Cornelisse CJ & Fleuren GJ 2005 High-resolution multi-parameter DNA flow cytometry enables detection of tumour and stromal cell subpopulations in paraffin-embedded tissues. *Journal of Pathology* **206** 233–241. (https://doi.org/10.1002/path.1765)

Corver WE, Middeldorp A, Ter Haar NT, Jordanova ES, van Puijenbroek M, van Eijk R, Cornelisse CJ, Fleuren GJ, Morreau H, Oosting J, *et al*. 2008 Genome-wide allelic state analysis on flow-sorted tumor fractions provides an accurate measure of chromosomal aberrations. *Cancer Research* **68** 10333–10340. (https://doi.org/10.1158/0008-5472.CAN-08-2665)

Corver WE, Ruano D, Weijers K, den Hartog WC, van Nieuwenhuizen MP, de Miranda N, van Eijk R, Middeldorp A, Jordanova ES, Oosting J, *et al*. 2012 Genome haploidisation with chromosome 7 retention in oncocytic follicular thyroid carcinoma. *PLoS ONE* **7** e38287. (https://doi.org/10.1371/journal.pone.0038287)

Corver WE, van WT, Molenaar K, Schrumpf M, van den Akker B, van ER, Ruano ND, Oosting J & Morreau H 2014 Near-haploidization significantly associates with oncocytic adrenocortical, thyroid, and parathyroid tumors but not with mitochondrial DNA mutations. *Genes, Chromosomes and Cancer* **53** 833–844. (https://doi.org/10.1002/gcc.22194)

de Vries MM, Celestino R, Castro P, Eloy C, Maximo V, van der Wal JE, Plukker JT, Links TP, Hofstra RM, Sobrinho-Simoes M, *et al*. 2012 RET/PTC rearrangement is prevalent in follicular Hurthle cell carcinomas. *Histopathology* **61** 833–843. (https://doi.org/10.1111/j.1365-2559.2012.04276.x)

Demeure MJ, Damsky CH, Elfman F, Goretzki PE, Wong MG & Clark OH 1992 Invasion by cultured human follicular thyroid cancer correlates with increased beta 1 integrins and production of proteases. *World Journal of Surgery* **16** 770–776. (https://doi.org/10.1007/BF02067383)

Dettori T, Frau DV, Lai ML, Mariotti S, Uccheddu A, Daniele GM, Tallini G, Faa G & Vanni R 2003 Aneuploidy in oncocytic lesions of the thyroid gland: diffuse accumulation of mitochondria within the cell is associated with trisomy 7 and progressive numerical chromosomal alterations. *Genes, Chromosomes and Cancer* **38** 22–31. (https://doi.org/10.1002/gcc.10238)

Di Cristofaro J, Silvy M, Lanteaume A, Marcy M, Carayon P & De Micco C 2006 Expression of tpo mRNA in thyroid tumors: quantitative PCR analysis and correlation with alterations of ret, Braf, ras and pax8 genes. *Endocrine-Related Cancer* **13** 485–495. (https://doi.org/10.1677/erc.1.01164)

Duijf PH, Schultz N & Benezra R 2013 Cancer cells preferentially lose small chromosomes. *International Journal of Cancer* **132** 2316–2326. (https://doi.org/10.1002/ijc.27924)

Erickson LA, Jalal SM, Goellner JR, Law ME, Harwood A, Jin L, Roche PC & Lloyd RV 2001 Analysis of Hurthle cell neoplasms of the thyroid by interphase fluorescence in situ hybridization. *American Journal of Surgical Pathology* **25** 911–917. (https://doi.org/10.1097/00000478-200107000-00009)

Evangelisti C, de BD, Kurelac I, Ceccarelli C, Prokisch H, Meitinger T, Caria P, Vanni R, Romeo G, Tallini G, *et al*. 2015 A mutation screening of oncogenes, tumor suppressor gene TP53 and nuclear encoded mitochondrial complex I genes in oncocytic thyroid tumors. *BMC Cancer* **15** 157. (https://doi.org/10.1186/s12885-015-1122-3)

Flint A & Lloyd RV 1990 Hurthle-cell neoplasms of the thyroid gland. *Pathology Annual* **25** 37–52.

Ganly I, Ricarte FJ, Eng S, Ghossein R, Morris LG, Liang Y, Socci N, Kannan K, Mo Q, Fagin JA, *et al*. 2013 Genomic dissection of Hurthle cell carcinoma reveals a unique class of thyroid malignancy. *Journal of Clinical Endocrinology and Metabolism* **98** E962–E972. (https://doi.org/10.1210/jc.2012-3539)

Geldof AA, Versteegh LRT, Van Mourik JC, Rooimans MA, Arwert F, Hermsen MA, Schadee-Eestermans IL, van Dongen GA, van der Valk P,van der Clement EHP, *et al*. 2001 Clonally related but phenotypically divergent human cancer cell lines derived from a single follicular thyroid cancer recurrence (TT2609). *Thyroid* **11** 909–917. (https://doi.org/10.1089/105072501753210966)

Goretzki PE, Frilling A, Simon D & Roeher HD 1990 Growth regulation of normal thyroids and thyroid tumors in man. *Recent Results in Cancer Research* **118** 48–63. (https://doi.org/10.1007/978-3-642-83816-3_6)

Guo Z, Kozlov S, Lavin MF, Person MD & Paull TT 2010 ATM activation by oxidative stress. *Science* **330** 517–521. (https://doi.org/10.1126/science.1192912)

Hogan T, Jing JY, Williams HJ, Altaha R, Xiaobing L & Qi H 2009 Oncocytic, focally anaplastic, thyroid cancer responding to erlotinib. *Journal of Oncology Pharmacy Practice* **15** 111–117. (https://doi.org/10.1177/1078155208101212)

Ju YS, Alexandrov LB, Gerstung M, Martincorena I, Nik-Zainal S, Ramakrishna M, Davies HR, Papaemmanuil E, Gundem G, Shlien A, *et al*. 2014 Origins and functional consequences of somatic mitochondrial DNA mutations in human cancer. *eLife* **3** e02935. (https://doi.org/10.7554/eLife.02935)

Kasaian K, Chindris AM, Wiseman SM, Mungall KL, Zeng T, Tse K, Schein JE, Rivera M, Necela BM, Kachergus JM, *et al*. 2015 MEN1 mutations in Hurthle cell (oncocytic) thyroid carcinoma. *Journal of Clinical Endocrinology and Metabolism* **100** E611–E615. (https://doi.org/10.1210/jc.2014-3622)

Landa I, Ganly I, Chan TA, Mitsutake N, Matsuse M, Ibrahimpasic T, Ghossein RA & Fagin JA 2013 Frequent somatic TERT promoter mutations in thyroid cancer: higher prevalence in advanced forms of the disease. *Journal of Clinical Endocrinology and Metabolism* **98** E1562–E1566. (https://doi.org/10.1210/jc.2013-2383)

Larman TC, DePalma SR, Hadjipanayis AG, Protopopov A, Zhang J, Gabriel SB, Chin L, Seidman CE, Kucherlapati R & Seidman JG 2012 Spectrum of somatic mitochondrial mutations in five cancers. *PNAS* **109** 14087–14091. (https://doi.org/10.1073/pnas.1211502109)

Lee J, Ham S, Lee MH, Kim SJ, Park JH, Lee SE, Chang JY, Joung KH, Kim TY, Kim JM, *et al*. 2015 Dysregulation of Parkin-mediated mitophagy in thyroid Hurthle cell tumors. *Carcinogenesis* **36** 1407–1418. (https://doi.org/10.1093/carcin/bgv122)

Lee S, Kopp F, Chang TC, Sataluri A, Chen B, Sivakumar S, Yu H, Xie Y & Mendell JT 2016 Noncoding RNA NORAD regulates genomic stability by sequestering PUMILIO proteins. *Cell* **164** 69–80. (https://doi.org/10.1016/j.cell.2015.12.017)

Maximo V, Botelho T, Capela J, Soares P, Lima J, Taveira A, Amaro T, Barbosa AP, Preto A, Harach HR, *et al*. 2005 Somatic and germline mutation in GRIM-19, a dual function gene involved in mitochondrial metabolism and cell death, is linked to mitochondrion-rich (Hurthle cell) tumours of the thyroid. *British Journal of Cancer* **92** 1892–1898. (https://doi.org/10.1038/sj.bjc.6602547)

Maximo V, Rios E & Sobrinho-Simoes M 2014 Oncocytic lesions of the thyroid, kidney, salivary glands, adrenal cortex, and parathyroid glands. *International Journal of Surgical Pathology* **22** 33–36. (https://doi.org/10.1177/1066896913517938)

McLeod MK, Thompson NW, Hudson JL, Gaglio JA, Lloyd RV, Harness JK, Nishiyama R & Cheung PS 1988 Flow cytometric measurements of nuclear DNA and ploidy analysis in Hurthle cell neoplasms of the thyroid. *Archives of Surgery* **123** 849–854. (https://doi.org/10.1001/archsurg.1988.01400310063010)

Mirebeau-Prunier D, Le PS, Jacques C, Fontaine JF, Gueguen N, Boutet-Bouzamondo N, Donnart A, Malthiery Y & Savagner F 2013 Estrogen-related receptor alpha modulates lactate dehydrogenase activity in thyroid tumors. *PLoS ONE* **8** e58683. (https://doi.org/10.1371/journal.pone.0058683)

Mond M, Alexiadis M, Fuller PJ & Gilfillan C 2014 Mutation profile of differentiated thyroid tumours in an Australian urban population. *Internal Medicine Journal* **44** 727–734. (https://doi.org/10.1111/imj.12476)

Musholt PB, Musholt TJ, Morgenstern SC, Worm K, Sheu SY & Schmid KW 2008 Follicular histotypes of oncocytic thyroid carcinomas do not carry mutations of the BRAF hot-spot. *World Journal of Surgery* **32** 722–728. (https://doi.org/10.1007/s00268-007-9431-6)

Ohta K, Pang XP, Berg L & Hershman JM 1997 Growth inhibition of new human thyroid carcinoma cell lines by activation of adenylate cyclase through the beta-adrenergic receptor. *Journal of Clinical Endocrinology and Metabolism* **82** 2633–2638.

Oosting J, Lips EH, van Eijk R, Eilers PH, Szuhai K, Wijmenga C, Morreau H & van Wezel T 2007 High-resolution copy number analysis of paraffin-embedded archival tissue using SNP BeadArrays. *Genome Research* **17** 368–376. (https://doi.org/10.1101/gr.5686107)

Pagan M, Kloos RT, Lin CF, Travers KJ, Matsuzaki H, Tom EY, Kim SY, Wong MG, Stewart AC, Huang J, *et al*. 2016 The diagnostic application of RNA sequencing in patients with thyroid cancer: an analysis of 851 variants and 133 fusions in 524 genes. *BMC Bioinformatics* **17** (Supplement 1) S6. (https://doi.org/10.1186/s12859-015-0849-9)

Qasem E, Murugan AK, Al-Hindi H, Xing M, Almohanna M, Alswailem M & Alzahrani AS 2015 TERT promoter mutations in thyroid cancer: a report from a Middle Eastern population. *Endocrine-Related Cancer* **22** 901–908. (https://doi.org/10.1530/ERC-15-0396)

Ribeiro FR, Meireles AM, Rocha AS & Teixeira MR 2008 Conventional and molecular cytogenetics of human non-medullary thyroid carcinoma: characterization of eight cell line models and review of

the literature on clinical samples. *BMC Cancer* **8** 371. (https://doi.org/10.1186/1471-2407-8-371)

Roque L, Serpa A, Clode A, Castedo S & Soares J 1999 Significance of trisomy 7 and 12 in thyroid lesions with follicular differentiation: a cytogenetic and in situ hybridization study. *Laboratory Investigation* **79** 369–378.

Salmon I, Gasperin P, Remmelink M, Rahier I, Rocmans P, Pasteels JL, Heimann R & Kiss R 1993 Ploidy level and proliferative activity measurements in a series of 407 thyroid tumors or other pathologic conditions. *Human Pathology* **24** 912–920. (https://doi.org/10.1016/0046-8177(93)90143-5)

Samuni Y, Goldstein S, Dean OM & Berk M 2013 The chemistry and biological activities of N-acetylcysteine. *Biochimica et Biophysica Acta* **1830** 4117–4129. (https://doi.org/10.1016/j.bbagen.2013.04.016)

Savagner F, Franc B, Guyetant S, Rodien P, Reynier P & Malthiery Y 2001 Defective mitochondrial ATP synthesis in oxyphilic thyroid tumors. *Journal of Clinical Endocrinology and Metabolism* **86** 4920–4925. (https://doi.org/10.1210/jcem.86.10.7894)

Schulten HJ, Salama S, Al-Ahmadi A, Al-Mansouri Z, Mirza Z, Al-Ghamdi K, Al-Hamour OA, Huwait E, Gari M, Al-Qahtani MH, *et al*. 2013 Comprehensive survey of HRAS, KRAS, and NRAS mutations in proliferative thyroid lesions from an ethnically diverse population. *Anticancer Research* **33** 4779–4784.

Sinno S, Choucair M, Nasrallah M, Wadi L, Jabbour MN & Nassif S 2016 Activating BRAF mutations detected in mixed hurthle cell carcinoma and multifocal papillary carcinoma of the thyroid gland: report of an unusual case and review of the literature. *International Journal of Surgical Pathology* **24** 519–524. (https://doi.org/10.1177/1066896916639377)

Spambalg D, Sharifi N, Elisei R, Gross JL, Medeiros-Neto G & Fagin JA 1996 Structural studies of the thyrotropin receptor and Gs alpha in human thyroid cancers: low prevalence of mutations predicts infrequent involvement in malignant transformation. *Journal of Clinical Endocrinology and Metabolism* **81** 3898–3901.

Stankov K, Biondi A, D'Aurelio M, Gasparre G, Falasca A, Romeo G & Lenaz G 2006 Mitochondrial activities of a cell line derived from thyroid Hurthle cell tumors. *Thyroid* **16** 325–331. (https://doi.org/10.1089/thy.2006.16.325)

Tallini G, Hsueh A, Liu S, Garcia-Rostan G, Speicher MR & Ward DC 1999 Frequent chromosomal DNA unbalance in thyroid oncocytic (Hurthle cell) neoplasms detected by comparative genomic hybridization. *Laboratory Investigation* **79** 547–555.

Vindelov LL, Christensen IJ & Nissen NI 1983 A detergent-trypsin method for the preparation of nuclei for flow cytometric DNA analysis. *Cytometry* **3** 323–327. (https://doi.org/10.1002/cyto.990030503)

Wada N, Duh QY, Miura D, Brunaud L, Wong MG & Clark OH 2002 Chromosomal aberrations by comparative genomic hybridization in Hürthle cell thyroid carcinomas are associated with tumor recurrence. *Journal of Clinical Endocrinology and Metabolism* **87** 4595–4601. (https://doi.org/10.1210/jc.2002-020339)

Wagle N, Grabiner BC, Van Allen EM, Amin-Mansour A, Taylor-Weiner A, Rosenberg M, Gray N, Barletta JA, Guo Y, Swanson SJ, *et al*. 2014 Response and acquired resistance to everolimus in anaplastic thyroid cancer. *New England Journal of Medicine* **371** 1426–1433. (https://doi.org/10.1056/NEJMoa1403352)

Wei S, LiVolsi VA, Montone KT, Morrissette JJ & Baloch ZW 2015 PTEN and TP53 mutations in oncocytic follicular carcinoma. *Endocrine Pathology* **26** 365–369. (https://doi.org/10.1007/s12022-015-9403-6)

Wei S, LiVolsi VA, Brose MS, Montone KT, Morrissette JJ & Baloch ZW 2016 STK11 mutation identified in thyroid carcinoma. *Endocrine Pathology* **27** 65–69. (https://doi.org/10.1007/s12022-015-9411-6)

Zhou S, Kachhap S, Sun W, Wu G, Chuang A, Poeta L, Grumbine L, Mithani SK, Chatterjee A, Koch W, *et al*. 2007 Frequency and phenotypic implications of mitochondrial DNA mutations in human squamous cell cancers of the head and neck. *PNAS* **104** 7540–7545. (https://doi.org/10.1073/pnas.0610818104)

Zielke A, Tezelman S, Jossart GH, Wong M, Siperstein AE, Duh QY & Clark OH 1998 Establishment of a highly differentiated thyroid cancer cell line of Hürthle cell origin. *Thyroid* **8** 475–483. (https://doi.org/10.1089/thy.1998.8.475)

Received in final form 29 September 2017
Accepted 24 October 2017
Accepted Preprint published online 24 October 2017